

Zeitschrift: IABSE proceedings = Mémoires AIPC = IVBH Abhandlungen
Band: 6 (1982)
Heft: P-54: Widths of initial cracks in concrete tension flanges of composite beams

Artikel: Widths of initial cracks in concrete tension flanges of composite beams
Autor: Randl, Ewald / Johnson, Roger Paul
DOI: <https://doi.org/10.5169/seals-36660>

Nutzungsbedingungen

Die ETH-Bibliothek ist die Anbieterin der digitalisierten Zeitschriften auf E-Periodica. Sie besitzt keine Urheberrechte an den Zeitschriften und ist nicht verantwortlich für deren Inhalte. Die Rechte liegen in der Regel bei den Herausgebern beziehungsweise den externen Rechteinhabern. Das Veröffentlichen von Bildern in Print- und Online-Publikationen sowie auf Social Media-Kanälen oder Webseiten ist nur mit vorheriger Genehmigung der Rechteinhaber erlaubt. [Mehr erfahren](#)

Conditions d'utilisation

L'ETH Library est le fournisseur des revues numérisées. Elle ne détient aucun droit d'auteur sur les revues et n'est pas responsable de leur contenu. En règle générale, les droits sont détenus par les éditeurs ou les détenteurs de droits externes. La reproduction d'images dans des publications imprimées ou en ligne ainsi que sur des canaux de médias sociaux ou des sites web n'est autorisée qu'avec l'accord préalable des détenteurs des droits. [En savoir plus](#)

Terms of use

The ETH Library is the provider of the digitised journals. It does not own any copyrights to the journals and is not responsible for their content. The rights usually lie with the publishers or the external rights holders. Publishing images in print and online publications, as well as on social media channels or websites, is only permitted with the prior consent of the rights holders. [Find out more](#)

Download PDF: 22.08.2025

ETH-Bibliothek Zürich, E-Periodica, <https://www.e-periodica.ch>

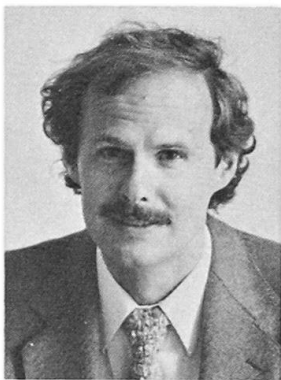
Widths of Initial Cracks in Concrete Tension Flanges of Composite Beams

Largeur des premières fissures des semelles en béton de poutres mixtes sous traction

Erstrissbreiten in Beton-Zuggurten von Verbundträgern

Ewald RANDL

Univ. Doz., Dr. techn.
Techn. University of Graz
Graz, Austria



E. Randl graduated as civil engineer from Techn. University of Graz and worked there since 1967 at the Institute of Steel, Wooden, and Plate and Shell Structures with Professors Beer and Resinger. He was concerned with design, checking and inspection of big Austrian composite bridges and is member of relevant Austrian Standard Committees.

Roger Paul JOHNSON

Prof. of Civil Engineering
University of Warwick
Coventry, England



R. P. Johnson worked for Ove Arup and Partners and lectured in engineering at Cambridge University before moving to the University of Warwick in 1971. He has authored two books and many research papers on composite construction and is a member of the European Joint Committee for Composite Structures.

SUMMARY

The first transverse cracks that occur in lightly-reinforced concrete slabs forming tension flanges of composite beams are found to be significantly wider than is predicted by existing methods. It is shown that this results from the flexibility of the shear connection, not from the shrinkage of the concrete. Predictions of the widths of these cracks are shown to agree with the test data, and simplified equations are given for use in design.

RÉSUMÉ

La largeur des premières fissures apparaissant dans les semelles en béton faiblement armé de poutres mixtes sous traction est beaucoup plus grande que ne le prédisent les méthodes de calcul actuelles. L'article montre que cela est dû à la flexibilité des joints de cisaillement et non pas au retrait du béton. La méthode de calcul de la largeur de ces fissures est confirmée par les résultats d'essai, et des équations simplifiées sont proposées pour le calcul du projet.

ZUSAMMENFASSUNG

Die Rissbreiten der querliegenden Erstrisse in schwach bewehrten Beton-Zuggurten von Verbundträgern erscheinen viel weiter als sie nach bestehenden Methoden errechnet werden. Es wird gezeigt, dass dies durch die Nachgiebigkeit der Verdübelung und nicht durch Schwinden des Betons begründet ist. Berechnungsmethoden, die durch Versuchsergebnisse bestätigt werden, und einfache Rissbreitenformeln für die praktische Bemessung werden gezeigt.

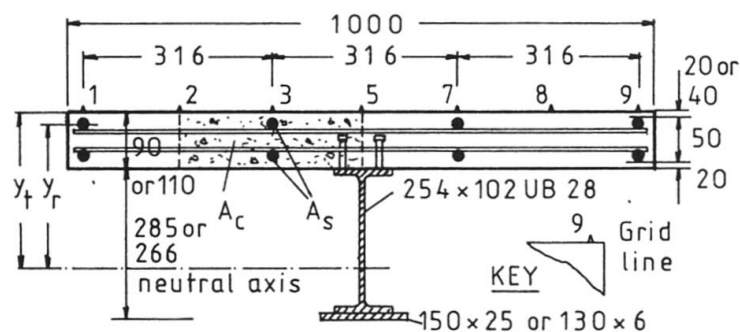
1. INTRODUCTION

In codes of practice for continuous composite beams of steel and concrete in both bridges and buildings, limits are specified for the widths of cracks in the slab at the serviceability limit state. Current methods for the prediction of these widths in negative (hogging) moment regions [1,2,3] are based on rules developed from extensive research on cracking in reinforced concrete members, on the assumption that the behaviour of the concrete flange of a composite member is similar. When studying this assumption it is necessary to relate the work to a particular method of crack-width prediction, because current methods give a wide range of results [4].

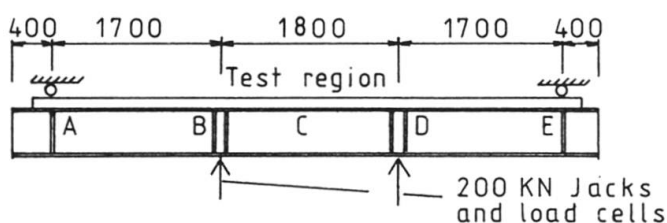
Roik and Ehler found [5] that Reference [3] gave satisfactory prediction of the cracking observed in their tests on composite plate girders, conducted in the open air, but did not pay special attention to initial crack widths. Johnson and Allison tested in a laboratory eight composite beams of the proportions used in buildings, and made about 8000 measurements of crack width. They found [6,7] that the results did not agree well with the predictions of BS 5400:Part 5[2], particularly when crack widths were less than about 0.2 mm. They attributed this partly to the effects of shrinkage (normally neglected in Reference[2]), but also found that several relationships well-established for reinforced concrete beams did not hold for flanges of composite beams.

Widths of cracks are strongly influenced by the mean longitudinal strain at the surface of the concrete slab, $\bar{\epsilon}$, and by the local ratio of area of reinforcement to area of concrete, ρ . It is usually assumed that once cracks have formed in reinforced concrete, their mean width \bar{w} is proportional to $\bar{\epsilon}$. Johnson and Allison found this to be so when $\bar{\epsilon} > 0.001$, but only true at lower values of $\bar{\epsilon}$ when the reinforcement ratio ρ was high. They based their method of prediction on the assumption $\bar{w} \propto \bar{\epsilon}$, and recognised that it did not apply to the first few cracks that form (at $\bar{\epsilon} < 0.001$) in a slab with a low reinforcement ratio. The initial cracking observed in their tests is analysed and explained in this paper.

The importance of this subject is shown by recent inspections of deck slabs in composite bridges in Austria. Many examples have been found of local damage in regions of tension near internal supports, caused by wide cracks. Reinforcement ratios in these regions were typically 0.3% to 0.6%.



(a) TYPICAL CROSS SECTION



(b) TYPICAL ELEVATION

Fig.1 Test specimens

2. RESULTS OF TESTS ON COMPOSITE BEAMS

A typical cross section and elevation of the beams is shown in Figure 1. They were numbered UC1 to UC8. Each one was subjected to slowly increasing load over a period of one or two days, until the maximum bending moment was about 80% of the value at which the steel beam was expected to yield. Longitudinal strains and crack widths were measured after each load increment along grid lines that were closely spaced over the test region, which was 1.8 m long and 1.0 m wide. Strains in the steel beam, slip, uplift, rotations, and deflections were also measured [6,7]. This paper considers only the region between

grid lines 2 and 8 (Figure 1), in which the reinforcement ratio is given by $\rho = A_s/A_c$. The ratio for the outer regions is higher. Values of ρ and other relevant data are given in Table 1. The diameter ϕ of the longitudinal bars was constant for each beam.

Test	ϕ	ρ	f_{cu}	f_t	f_{bt}	ϵ_{sh}	α_e	ϕ_c	f_y	Y_t/Y_r
	mm	%	N/mm ²	N/mm ²	N/mm ²	$\times 10^{-6}$			N/mm ²	
UC1	10	1.10	39.6	3.2	3.60	440	6.6	5.2	478	1.10
UC2	12	0.80	38.8	3.1	3.50	401	6.6	5.0	437	1.11
UC3	12	0.80	40.1	3.4	3.84	440	6.6	5.2	437	1.11
UC4	12	0.65	51.6	3.8	4.63	248	6.0	3.2	437	1.19
UC5	12	0.80	24.8	2.5	2.95	586	7.9	6.0	437	1.14
UC6	16	1.41	43.6	3.1	3.59	269	6.1	3.4	500	1.12
UC7	12	0.65	50.1	4.0	4.87	236	6.0	3.0	437	1.19
UC8	12	0.65	60.0	3.8	4.56	302	5.8	3.8	437	1.19

Table 1 Properties of material and test specimens

The properties f_{cu} , f_t and f_y of the materials were found by conventional tests [6]. The bending tensile strength f_{bt} was also required. This is known to depend on the stress gradient through the concrete specimen, and was calculated for these specimens from the stresses prior to cracking and the direct tensile strength f_t , using a formula due to Heilmann from Reference [8]. Modulus of rupture tests were carried out, but the results were not used (except in discussing results from beam UC5), as they correspond to one particular stress gradient. Modular ratios $\alpha_e (=E_s/E_c)$ were found assuming $E_s = 207 \text{ kN/mm}^2$ and using values of E_c calculated from measured cube strengths in accordance with BS 5400 [9].

The free shrinkage strain for each slab, ϵ_{sh} , was deduced from strain readings on five concrete prisms that were cured with the slab. The creep coefficients ϕ_c (ratio of creep strain to elastic strain) associated with this shrinkage were determined as follows. Both creep and shrinkage are influenced by the same partial coefficients for composition of the concrete and variation with time. These were deduced from the free shrinkage strains ϵ_{sh} . The other partial coefficients for creep were taken from Reference [9].

The tensile stress $\epsilon_{st}E_c$ at the top surface of the slab at the time of the test, due to restraint of this shrinkage by the steel beam, was calculated allowing for creep. The associated tensile strain (ϵ_{st}) was assumed to be present when zero readings were taken at the start of each test.

Typical results from three of the tests are shown in Figure 2. The mean strain for a grid line, $\bar{\epsilon}$, is the sum of ϵ_{st} and the mean of 19 readings taken to Demec discs placed along the line at 4 in (102mm) spacing, using an 8-in Demec gauge

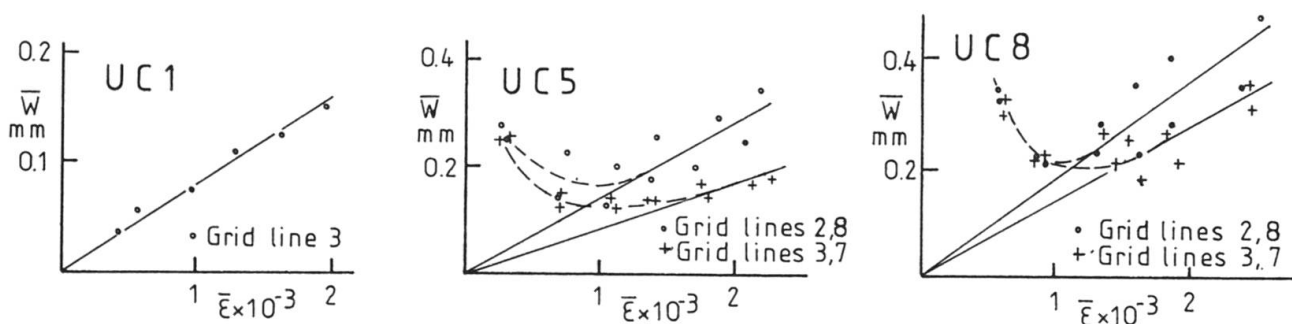


Fig.2 Mean crack widths and mean strain

and overlapping gauge lengths. The mean crack width \bar{w} is calculated from the widths of all the cracks crossing a grid line (of length 2.03 m), measured to the nearest 0.025 mm.

The data show that \bar{w} is proportional to $\bar{\epsilon}$ at high strains, but that in beams UC5 and UC8 the first few cracks to form were initially several times wider than would be predicted from the ratio $\bar{w}/\bar{\epsilon}$ at higher strains. These extra-wide initial cracks were observed in all the beams except UC1 and UC6.

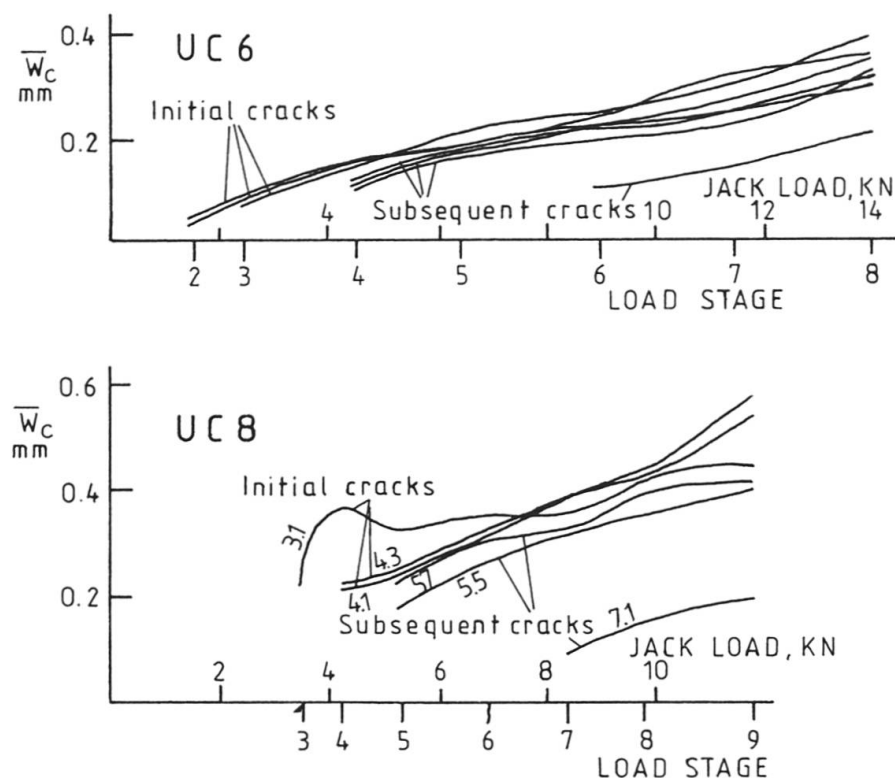


Fig.3 Changes in widths of cracks with increasing load

denotes the load stage at which it first appeared. Representative values of initial crack width \bar{w}_m were found as follows. Data were used only from the first two or three main cracks to form. These crossed the full width of the slab and were widely spaced, and so did not influence each other. The widths of the first crack were measured at two consecutive load stages. Subsequent cracks were measured only at the load stage when they first appeared, so have lower weight in the overall average.

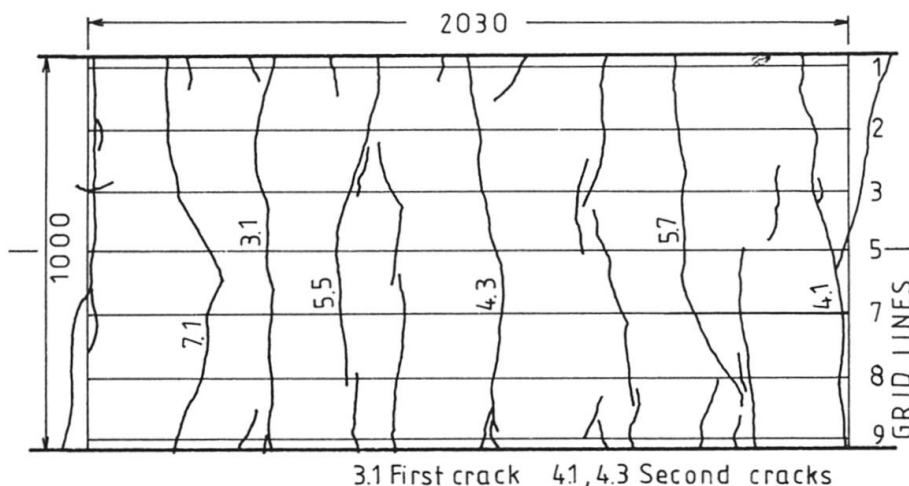


Fig.4 Test UC8. Plan of slab showing final crack pattern

Changes in the widths of cracks with increasing load are shown in Figure 3. Each line represents a particular crack, and \bar{w}_c is the mean of readings above and between bars. In UC6 the ratio of crack width to load is almost the same for subsequent cracks as for initial cracks; but in UC8 where the reinforcement ratio was lower, the first cracks remain the widest ones at the upper load stages, and the variation in crack width is much greater.

Initial cracking was studied closely in test UC8. The final cracking pattern in the test region is shown in Fig.4. The first digit of the number beside each crack

denotes the load stage at which it first appeared. Representative values of initial crack width \bar{w}_m were found as follows. Data were used only from the first two or three main cracks to form. These crossed the full width of the slab and were widely spaced, and so did not influence each other. The widths of the first crack were measured at two consecutive load stages. Subsequent cracks were measured only at the load stage when they first appeared, so have lower weight in the overall average.

The mean width "above bars" was found from measurements on lines 3 and 7. Data from lines 2, 5, and 8 were used for \bar{w}_m "between bars". Similar procedures were used for the other slabs. The results are given in Table 2. Comparison with Table 1 shows that initial crack width increases as ρ decreases.

3. PREDICTION OF INITIAL CRACK WIDTH

Test	σ_{s1}	σ_{s2}	w_{mr}	Above bars		Between bars	
				\bar{w}_m	\bar{w}_m/w_m	\bar{w}_m	\bar{w}_m/w_m
	N/mm ²	N/mm ²	mm	mm		mm	
UC1	-54	259	0.075	0.064	0.73	-	-
UC2	-54	356	0.149	0.144	0.84	0.181	0.86
UC3	-54	356	0.145	0.144	0.86	0.208	1.00
UC4	-15	477	0.175	0.206	0.91	0.254	0.92
UC5	-31	281	0.141	0.248	1.48	0.328	1.58
UC6	-8	196	0.058	0.088	1.26	0.136	1.24
UC7	-22	498	0.196	0.234	0.94	0.323	1.08
UC8	-33	494	0.168	0.253	1.18	0.293	1.13

Table 2 Observed and predicted results

A method of prediction due to Noakowski [8] is available for reinforced concrete members in axial tension. It agrees well with the results of tests by Falkner [10] on axially reinforced members with fixed ends subjected to falling temperature, and with measured crack widths from structures in service [8]. In applying it to composite members it is possible to correct for the curvature of the slab; but there remains the question of the influence of the shear connection on initial crack width.

This was resolved by analysing one of the test specimens (UC4) by linear partial-interaction theory, assuming that there was no longitudinal reinforcement in the slab, and that the first and only crack occurred at the centre of the test region, when the top-fibre tensile stress reached the bending tensile strength of the concrete, 5.3 N/mm². The effects of shear lag and shrinkage were neglected. The stiffness of each shear connector was taken as 65 kN/mm. This corresponds to the slip (0.8 mm) at 80% of the ultimate strength (65 kN) for typical stud connectors of the size used (16 mm diameter, 65 mm high), taking account of the cube strength of the concrete, 51.6 N/mm².

The calculation found the initial crack width to be 2.3 mm. This is about ten times the initial widths observed in the tests (0.21 mm and 0.25 mm), and shows that the influence of the shear connection (and of the steel beam) on the width of an initial crack is negligible in comparison with that of the reinforcement. The spacing of the studs in the other beams was similar to that in UC4 (225 mm), and no beam had less slab reinforcement than UC4, so the conclusion applies to all the beams.

It follows that the local loss of longitudinal stiffness of the slab caused by cracking has little influence on the stresses in the steel member. In the tests, the first crack to form was found to extend through the whole width and thickness of the concrete slab. In a determinate structure such as a composite cantilever, where there is no change of bending moment, such a crack will cause almost the whole of the tensile force resisted by the slab to be transferred to the reinforcement. It will be shown that a good prediction for the width of an initial crack is obtained by assuming that the stresses in the steel beam do not change. In the region near the crack where stress is transferred from concrete to reinforcement, plane sections do not remain plane in the composite member. A calculation based on that assumption will greatly under-estimate the stress in the reinforcement at the crack. In this respect, composite members differ from reinforced concrete members, in which the "shear connection" is very stiff.

If the proportion of slab reinforcement is low, the transfer of force on first cracking may cause the bars to yield. The crack may then be wider than is predicted by the method to be given here. The local loss of stiffness will then influence the loads on the shear connectors and the stresses in the steel beam, as it would if the slab were unreinforced.

In a redundant structure with sufficient slab reinforcement to prevent yield, initial cracking causes only a small and local reduction in the longitudinal

stiffness of the slab, and negligible shedding of bending moment from that region; so the assumption of no change in the stress in the steel beam has general applicability.

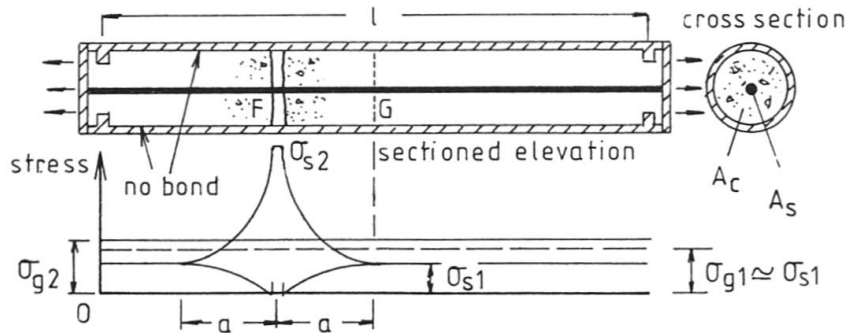


Fig.5 Axially restrained reinforced concrete member

For the test specimens, we assume that the shear connectors are effective along AB and DE (Figure 1), but that those along BD have no influence on an initial crack forming at C. The axial-stress equivalent of the situation in length BCD of the member is shown in Figure 5. The outer tube represents the steel member, which is attached

to the slab only at two points distant l apart, at which plane sections remain plane.

External forces and/or shrinkage cause the whole of the concrete initially to be at stress f_t , the axial tensile strength of the concrete. One crack then forms, at F, causing relief of tensile stress in the concrete over a length $2a$, and a rise in the stress in the reinforcement from σ_{s1} to a peak value σ_{s2} at the crack. The transfer length a depends on the relationship between the mean shear stress at the surface of the bar, τ , and the slip relative to the concrete, s .

In theory, the stress σ_{s1} and the initial stress σ_{g1} and the final stress σ_{g2} in the tube are all different, as shown, but when $a \ll l$ and there are no other cracks, all three stresses can be assumed to be equal.

Noakowski [8] assumed that

$$\tau = 0.19 k_1 f_{cu} s^n \quad (1)$$

where k_1 is a constant that depends on the quality of the bond or interlock between the reinforcing bars and the concrete. His result for the mean width at the surface of a bar of an initial crack is (in mm units):

$$w_{mr} = \left[\frac{1+n}{2^2-n} \cdot \frac{\phi \sigma_{s2} (\sigma_{s2} - \sigma_{s1})}{0.19 k_1 f_{cu} E_s} \right]^{1/(1-n)} \quad (2)$$

For deformed bars, n is taken as 0.16 and the result becomes

$$w_{mr} = 1.584 \left[\phi \sigma_{s2} (\sigma_{s2} - \sigma_{s1}) / k_1 f_{cu} E_s \right]^{0.862} \quad (3)$$

4. APPLICATION TO COMPOSITE BEAMS UC1 TO UC8

4.1 General

First, w_{mr} is calculated at the surface of a reinforcing bar in the upper layer (Figure 1(a)). Surface crack widths w_m are then predicted at grid lines above bars and midway between bars, taking account of the curvature of the member and the influence of distance to the nearest bar in the tensile stress in concrete near a crack. Account is taken of the initial stresses in the member due to the restrained shrinkage of the concrete slab. The calculated stresses for beam UC7 are shown in Figure 6.

It is assumed that external load is increased from zero until either the total concrete stress at the level of the upper reinforcing bar reaches the direct tensile strength f_t , or the tensile stress at the top surface of the slab reaches

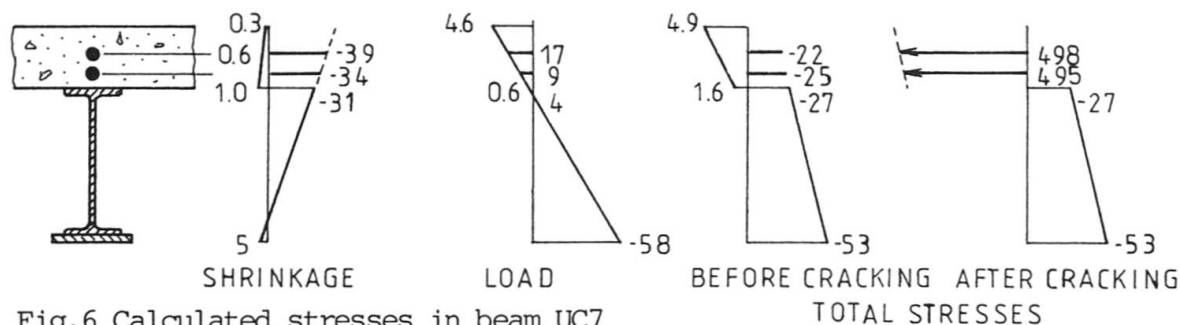


Fig.6 Calculated stresses in beam UC7

the bending tensile strength f_{bt} . The concrete then cracks, and the whole of the tensile force thus released is transferred to the two reinforcing bars, without any change in the curvature of the member or in the stresses in the steel beam.

It was found that the strength f_{bt} determines the cracking load for the three beams with 110-mm slabs (UC4, 7 and 8), and that cracking of the five beams with 90-mm slabs is determined by f_t .

Figure 6 shows that in beam UC7 the change in stress $\sigma_{s2} - \sigma_{s1}$ is 520 N/mm² for both bars. The stress σ_{s2} is taken as 498 N/mm² because w_{mr} is calculated at the surface of the upper bar. Values for the other beams are given in Table 2.

The stresses after cracking, σ_{s2} , exceed the yield stress f_y by about 10% in beams UC4, 7 and 8. It will be shown that this did not appear to cause extra widening of the cracks, probably because these high-yield bars do not have a clearly defined yield point.

4.2. The bond-slip relationship

No bond tests were done for these bars, so the constant k_1 in equations (1) and (3) was found in another way, assuming it to be the same for all the tests. It was deduced [7] from the fully-developed cracking patterns for mean strains exceeding 0.001 that the best prediction for the mean surface crack width above the bars was

$$w_m = (1.33c + 0.037\phi/\rho) \epsilon_m \quad (4)$$

where c is the concrete cover to the bars. This is the European, German, and British formulae [11, 12, 13], which give for this situation

$$w_m/\epsilon_m = f(c) + k_2 k_3 \phi/\rho \quad (5)$$

where k_2 relates to crack spacing and k_3 to the stress distribution in the concrete between cracks.

If σ_{ct} and σ_{cb} are the stresses at the top and bottom surfaces of the slab just before cracking, k_3 is given [11] by

$$k_3 = (\sigma_{ct} + \sigma_{cb})/8 \sigma_{ct} \quad (6)$$

The values of k_3 for the eight beams ranged from 0.16 to 0.20, with a mean of 0.184. By analogy between equations (4) and (5), $k_2 k_3 = 0.037$, so that $k_2 = 0.037/0.184 = 0.20$.

Related pairs of values of k_1 and k_2 can be deduced from crack-width formulae and associated bond tests, such as in References [8] and [11]; for example:

$$\begin{array}{ll} \text{for very weak bond:} & k_2 = 0.8, \quad k_1 = 1.0 \\ \text{for good bond:} & k_2 = 0.4, \quad k_1 = 2.0. \end{array}$$

As the bond strength diminishes ($k_1 \rightarrow 0$) the crack spacing becomes very wide ($k_2 \rightarrow \infty$), and vice versa, so the relationship between k_1 and k_2 can be assumed to be $k_1 k_2 = \text{constant}$. The constant for the results above is 0.8; so when $k_2 = 0.2$, k_1 should be about 4. Good agreement between theory and tests was obtained by

assuming $k_1=3.5$ here. This value implies very good shear transfer between concrete and reinforcement, as may be expected from deformed bars and slabs with the high mean cube strength of 44 N/mm^2 cast in a laboratory.

The calculated values w_{mr} are given in Table 2. In equation (3), E_s relates to reinforcement and was taken as 200 kN/mm^2 .

4.3 Crack width at the surface of the slab

Two corrections to w_{mr} are necessary. First, the crack width should be multiplied by y_t/y_r to allow for curvature of the beam, where y_t and y_r are the depths to the neutral axis of the cracked section shown in Figure 1. Their ratios are given in Table 1.

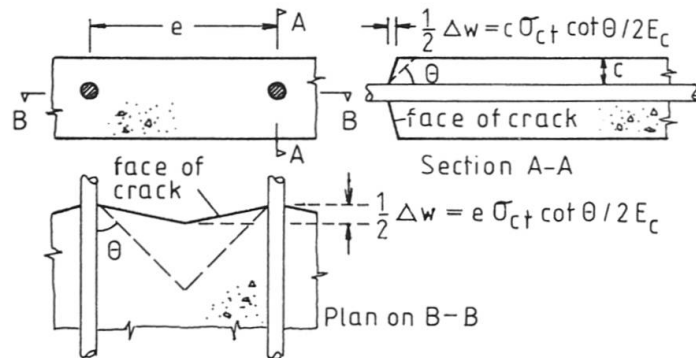


Fig.7 Increase in crack width due to distance to nearest bar

$$\begin{aligned} \Delta w &= c \sigma_{ct} \cot \theta / E_c && \text{above bars} \\ \Delta w &= e \sigma_{ct} \cot \theta / E_c && \text{between bars} \end{aligned}$$

where e is the lateral spacing of the reinforcing bars.

There is also an increase in width (Δw , say) due to the reduction in the tensile stress in the slab in the region close to the crack. This region is assumed to be defined by the angle of spread, θ , shown in Figure 7. This is usually assumed to lie between 30° and 45° , and is here taken as 37.5° . If σ_{ct} is the stress at the top surface of the slab in absence of cracking, and this stress is assumed to have fallen to zero over a length of surface defined by θ , then from Figure 7,

$$\left. \begin{aligned} \Delta w &= c \sigma_{ct} \cot \theta / E_c \\ \Delta w &= e \sigma_{ct} \cot \theta / E_c \end{aligned} \right\} \quad (7)$$

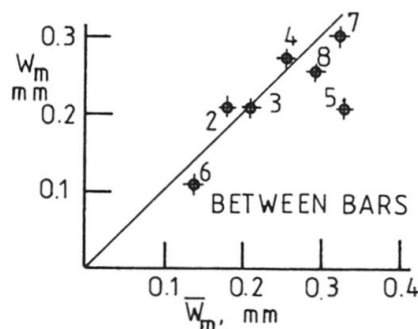
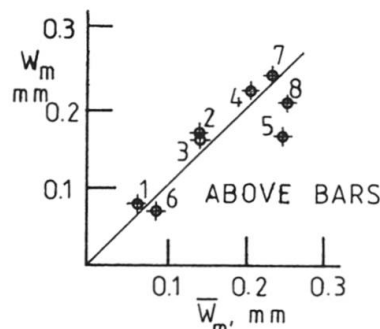


Fig.8 Observed and predicted crack widths

The crack width at the surface is therefore

$$w_m = w_{mr} y_t / y_r + \Delta w \quad (8)$$

The predicted values of w_m are shown in Figure 8 and are used to calculate the ratios \bar{w}_m / w_m given in Table 2.

The agreement between theory and test is good for all the beams except UC 5. It is suspected that the measured direct tensile strength for this beam (mean from three split-tensile tests) was low in relation to the tensile strength of the slab itself. The bending tensile strength predicted from f_t (Table 1) is 2.95 N/mm^2 , which is much lower than the mean result from the modulus of rupture tests, 3.8 N/mm^2 . If this last value had been used in the prediction of w_m , the ratios \bar{w}_m / w_m for this beam would have been 1.09 and 1.22. When UC5 is excluded, the mean of the ratios \bar{w}_m / w_m in Table 2 is reduced from 1.07 to 1.00.

5. SIMPLIFIED DESIGN RULES

The preceding method for predicting w_m , the mean width of initial cracks, requires knowledge of the stresses σ_{s1} and σ_{s2} which are not normally calculated. Simpler but approximate methods of prediction are now developed, drawing on work by Hughes [14] on the similar problem of early thermal and shrinkage cracking in concrete walls.

5.1. Minimum reinforcement ratio to prevent yielding at a crack

For longitudinal equilibrium of the concrete and reinforcement over length FG in Figure 5,

$$A_s \sigma_{s2} = A_s \sigma_{s1} + A_c f_t.$$

$$\text{Putting } A_s/A_c = \rho, \quad \sigma_{s2} - \sigma_{s1} = f_t/\rho \quad (9)$$

If the steel reaches yield at the crack, $\sigma_{s2} = f_y$ and $\sigma_{s1} \ll \sigma_{s2}$, so the critical (minimum) reinforcement ratio is

$$\rho_{cr} \simeq f_t/f_y. \quad (10)$$

Account is taken of the variability of the tensile strength of concrete by using the value with a 5% probability of being exceeded, given in Reference [11] as

$$f_t = 0.39 f_{ck}^{2/3}$$

where f_{ck} is the cylinder strength. This is taken as $0.75 f_{cu}$, giving

$$\rho_{cr} = 0.32 f_{cu}^{2/3}/f_y. \quad (11)$$

For $f_y = 425 \text{ N/mm}^2$, ρ_{cr} ranges from 0.6% to 0.9% as f_{cu} increases from 20 to 40 N/mm^2 .

5.2. Relation between reinforcement ratio, bar size, and mean crack width

Equation (2) can be simplified by putting $n = 0$. This corresponds to the rigid-plastic relationship between bond stress and slip assumed by Hughes, and makes the equation dimensionally correct. A factor 1.35 is included in the revised equation so that both equations give the same result when $w_{mr} = 0.2 \text{ mm}$. Assuming $k_1 = 2.0$ (Section 4.2, above), equation (2) becomes

$$w_{mr} = 0.89 \phi \sigma_{s2} (\sigma_{s2} - \sigma_{s1}) / f_{cu} E_s. \quad (12)$$

For compatibility of strain at section G in Figure 5,

$$\sigma_{s1} = \alpha_e f_t + \epsilon_{sh} E_s \quad (13)$$

where α_e is the modular ratio and ϵ_{sh} is the free shrinkage strain of the concrete. Using equations (9) and (13) to eliminate σ_{s1} and σ_{s2} ,

$$\begin{aligned} w_{mr} &= 0.89 \phi [(f_t/\rho) + \alpha_e f_t + \epsilon_{sh} E_s] f_t / \rho f_{cu} E_s \\ &= 0.89 \phi [1 + \alpha_e \rho + \alpha_e \rho \epsilon_{sh} / \epsilon_u] f_t^2 / \rho^2 f_{cu} E_s \end{aligned} \quad (14)$$

where ϵ_u is the ultimate tensile strain of concrete, taken as f_t/E_c . Typically, $\alpha_e \rho \simeq 0.1$ and $\epsilon_{sh}/\epsilon_u \simeq 2$, so the value of the square bracket is about 1.3. The CEB/FIP expression [11] for mean tensile strength is

$$f_t = 0.3 f_{ck}^{2/3}.$$

Assuming $f_{ck} = 0.75 f_{cu}$ as before, and putting $E_s = 200 \text{ kN/mm}^2$, equation (14) becomes

$$w_{mr} = 3.55 \times 10^{-7} \phi f_{cu}^{1/3} / \rho^2. \quad (15)$$

To predict surface crack widths, this result can be used with equations (7) and (8) with σ_{ct} taken as the tensile strength f_t of the concrete. Further simplification is only possible with loss of accuracy. For a bar spacing e not exceeding about 300 mm , and for main girders (for which $y_t \simeq y_r$), the factor y_t/y_r and

the term Δw in equation (8) can together be assumed to increase w_{mr} by about 15%. The mean initial crack width midway between bars is then

$$w_m = 0.004 \phi f_{cu}^{1/3} / \rho^2 \quad (16)$$

with ρ now in per cent and f_{cu} in N/mm^2 . This result is shown in Figure 9 in a form convenient for use in practice. The dashed line shows (for example) that the predicted mean initial crack width is just below 0.4 mm when $\rho = 0.8\%$, $f_{cu} = 60 N/mm^2$, and 16-mm bars are used at a spacing of about 300 mm.

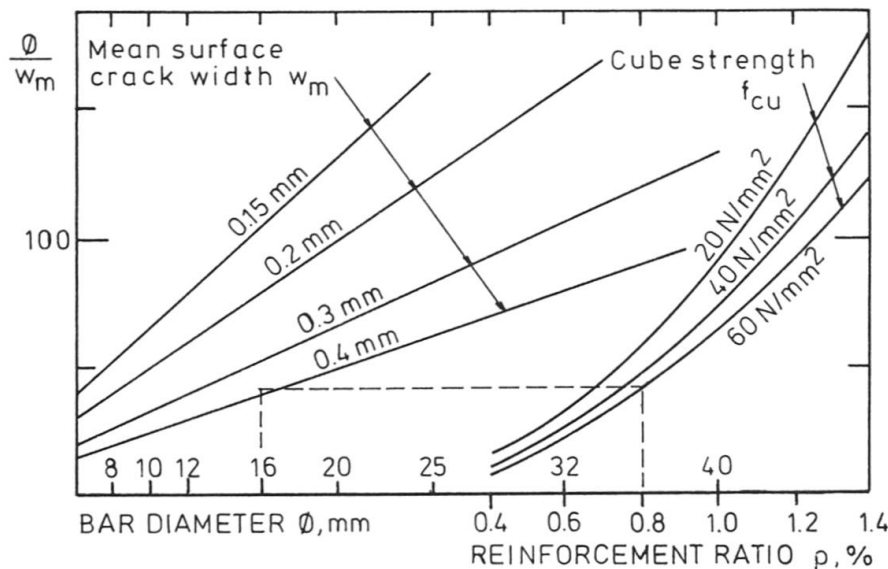


Fig.9 Mean initial crack width in terms of ϕ , f_{cu} and ρ

6. COMPARISON WITH EXISTING RULES FOR CRACK-WIDTH CONTROL

The current British design rules relate to crack widths with a 20% probability of being exceeded (w_{20} , say) and limiting values range from 0.1 mm to 0.3 mm, depending on environment. Initial crack widths are significant only if they exceed the value of w_{20} for which the slab reinforcement has been designed. No direct comparison can be made between w_{20} and w_m because the latter is a mean value. There are too few test data to enable 20% values to be predicted for initial cracks. For serviceability, w_m should be below w_{20} .

Trial calculations for slab reinforcement designed to a given value of w_{20} show that w_m sometimes exceeds w_{20} , particularly when the tensile stress in the reinforcement at working load is below about $200 N/mm^2$, and the local reinforcement ratio is low.

In 1972 it was recommended [15] that ρ should be at least 1%, to "assist with controlling ..cracking .. and provide a more favourable stress state in the longitudinal reinforcement". This proposal was related to the later stages of cracking. It takes no account of the strong influence of bar diameter on initial cracking, and is more conservative than the use of equation (11) for ρ_{cr} . The British codes give no value of ρ_{cr} , other than the minimum for main reinforcement in all slabs (normally 0.15%). Figure 9 shows that this is much too low in the situation considered here.

7. CONCLUSIONS

The first stage of cracking, when cracks are so widely spaced that there is no interaction between them, is rarely considered in current design practice, except in relation to early thermal and shrinkage cracking in walls. It is shown

above that when restraint from a compression zone is weak and the local reinforcement ratio is low (but still well above minimum values specified for slabs), initial cracks can be wider than is predicted by the methods in use for fully-developed crack patterns. These wide cracks have occurred in cantilevered as well as internal slabs in composite bridge decks in Austria in which most of the longitudinal reinforcement was placed in the slab to resist local wheel loads.

The cracks were wide because of insufficient local restraint to elastic recovery of the concrete. Shrinkage of the concrete reduces the external load at which the cracks first appear, but does not influence their width.

The use of light longitudinal reinforcement results from the common practices of spanning the deck slab transversely between main girders, and casting the slab in stages on unpropped steelwork. Stresses in longitudinal reinforcement at internal supports under service loading may then be as low as 100 N/mm^2 ; high enough to cause initial cracking but too low for existing rules for crack-width control to influence the detailing of the reinforcement.

In the United Kingdom, West Germany, Switzerland, and some other countries these rules are based on those for crack control in concrete bridges, where there is no need to consider initial cracking. The 1955 issue of the German code DIN 1078 required a minimum reinforcement ratio of 1% in tension regions of composite deck slabs. This rule was later removed, probably in the belief that the more recent crack-control clauses made it unnecessary.

The work reported here and the cracks in the Austrian bridges show that this belief is false. A requirement for a minimum reinforcement ratio of 0.9% in case of wide slabs has recently been added to the Austrian code. Equation (11) shows that 0.9% is sufficient to ensure that bars do not yield when the first crack forms; and Figure 9 gives an approximate relationship between the mean width of initial cracks, the reinforcement ratio, and other relevant variables, which suggests that 0.9% is sufficient to control initial cracking in composite main girders only when small-diameter bars are used.

NOTATION

A_c	cross-sectional area of concrete associated with bars of area A_s
A_s	cross-sectional area of reinforcing steel
a	transfer length on one side of a crack
c	concrete cover to top longitudinal reinforcement
E_c	elastic modulus of concrete for short-term loading
E_s	Young's modulus for steel reinforcement
e	spacing of longitudinal reinforcing bars
f_{bt}	bending tensile strength of concrete
f_{cu}	cube strength of concrete
f_t	direct tensile strength of concrete
f_y	yield strength of reinforcing steel
k	constant
s	longitudinal slip between reinforcing bar and adjacent concrete
\bar{w}	mean of measured crack widths along a grid line
w_m	predicted mean crack width at surface of slab
\bar{w}_m	mean of widths of initial cracks, above or midway between bars



- w_{mr} predicted mean crack width at surface of reinforcing bar
 y_r depth below top reinforcement of neutral axis when concrete is cracked
 y_t depth below top of slab of neutral axis when concrete is cracked
 α_e modular ratio, E_s/E_c
 $\bar{\epsilon}$ mean of measured surface strains along a grid line, including ϵ_{st}
 ϵ_m predicted mean surface strain, including ϵ_{st}
 ϵ_{sh} free shrinkage strain of slab
 ϵ_{st} calculated tensile strain due to restrained shrinkage of slab
 θ angle of spread of stress in concrete near a crack
 ρ local reinforcement ratio, A_s/A_c
 σ_c longitudinal stress in concrete
 σ_g longitudinal stress in steel girder or restraining member
 σ_{s1} longitudinal stress in reinforcing bar before cracking
 σ_{s2} longitudinal stress in reinforcing bar after cracking
 τ bond or shear stress at surface of reinforcing bar
 \varnothing diameter of reinforcing bar
 \varnothing_c creep coefficient

REFERENCES

1. CEB - ECCS - FIP - IABSE Joint Committee. Composite Structures (A Draft Model Code). Construction Press, London, 1981.
2. BS 5400:Part 5, Code of practice for design of composite bridges. British Standards Institution, London, 1979.
3. DIN 1045, Beton- und Stahlbetonbau, Bemessung und Ausführung. Beuth Verlag GmbH. Berlin 30, Dezember 1978.
4. SYGULA S. Vergleichende Untersuchungen über Biege- und Bruchformeln für Stahlbeton. Beton- und Stahlbetonbau, 5, 114-117, 1981.
5. EHLERT W. Grenzzustände schlanker Verbundträger. Tech. Report 81-7, Institut für Konstruktiven Ingenieurbau, Ruhr-Universität Bochum, 1981.
6. JOHNSON, R.P., ALLISON R.W. Shrinkage and tension stiffening in hogging moment regions of composite beams. Structural Engineer, 59B, 10-16, March 1981.
7. JOHNSON R.P., ALLISON R.W. Cracking in concrete tension flanges of composite T-beams. To be published, The Structural Engineer, 1982.
8. NOAKOWSKI P. Praxisgerechtes Verfahren für die Bemessung von Stahlbetonteilen bei Zwangsbeanspruchung. Beton- und Stahlbetonbau, 4, 77-82 and 5, 120-125, 1980.
9. BS 5400:Part 4, Code of practice for design of concrete bridges. British Standards Institution, London 1978.
10. FALKNER H. Zur Frage der Rißbildung durch Eigen- und Zwangsspannungen infolge Temperatur in Stahlbetonteilen. Deutscher Ausschuss für Stahlbeton, Heft 208, W. Ernst u. Sohn, 1969.
11. CEB - FIP Model Code for concrete structures. Comité Euro-International du Béton, Paris, 1978.
12. LEONHARDT F. Vorlesungen über Massivbau. 4. Teil, Springer, Berlin, 1977.
13. BEEBY A.W. The prediction of crack widths in hardened concrete. Structural Engineer, 57A, 9-17, Jan. 1979.
14. HUGHES B.P. Limit state theory for reinforced concrete, 233-244. Pitman, London, 1971.
15. FISHER J.W., DANIELS J.H., SLUTTER R.G. Continuous composite beams for bridges. Prelim. vol., 9th Congress, IABSE, 113-123, 1972.